Supporting Information

Impact of Phonon Dispersion on Nonlocal Electron-Phonon Couplings in Organic Semiconductors: The Naphthalene Crystal as a Case Study

Zeyi Tu,[†, ‡] Yuanping Yi,*[,†, ‡] Veaceslav Coropceanu,*[,§] and Jean-Luc Brédas[§]

[†]CAS Key Laboratory of Organic Solids, CAS Research/Education Center for Excellence in Molecular Sciences, Institute of Chemistry, Chinese Academy of Sciences, Beijing 100190, China

[‡]University of Chinese Academy Sciences, Beijing, 100049, China

[§]School of Chemistry and Biochemistry and Center for Organic Photonics and Electronics, Georgia Institute of Technology, Atlanta, Georgia 30332-0400, United States

* Corresponding authors. E-mail: ypyi@iccas.ac.cn, coropceanu@gatech.edu.

Influence of supercell sizes on phonon dispersions: The phonon dispersion curves calculated by using the normal unit cell, and $2\times1\times1$, $1\times2\times1$, and $1\times1\times2$ supercells are shown in Figure S1. For the normal unit cell, imaginary frequencies appear in all directions but the Γ-B direction (corresponding to the *a*-axis). Replication of the unit cell along the *a*-axis (the $2\times1\times1$ supercell) hardly influences the phonon dispersion profile. In contrast, when the unit cell is replicated along the *b*-axis or *c*-axis (the $1\times2\times1$ or $1\times1\times2$ supercell), the frequencies for both acoustic and optical phonons are significantly changed for wave vectors containing the Γ-Y or Γ-Z component (corresponding to the *b*- or *c*-axis). The imaginary frequencies are eliminated along the Γ-Y and Γ-A directions or along the Γ-Z and Γ-D directions. Then, to eliminate imaginary frequencies in the whole first Brillouin zone, the $1\times2\times2$ supercell (replication of the unit cell along both the *b*- and *c*-axes) is used and "exact" (no imaginary frequencies) phonon dispersion curves are obtained (see Figure 2). The influence of the replication directions can be rationalized in terms of the closest inter-atomic distances between adjacent equivalent molecules in the crystal (6.75, 2.86, and 2.62 Å along the *a*-, *b*-, and *c*-axis, respectively, see Figure S2). Owing to the short contacts along the *b*- and *c*-axes, more than one displaced atom can induce forces via intra- or inter-molecular interactions (see Figure S2), which will result in an incorrect evaluation of the phonon frequencies via the Parlinski-Li-Kawazoe method.[1]

(1) Parlinski, K.; Li, Z. Q.; Kawazoe, Y. First-Principles Determination of the Soft Mode in Cubiczro2. Phys. Rev. Lett. 1997, 78, 4063-4066.

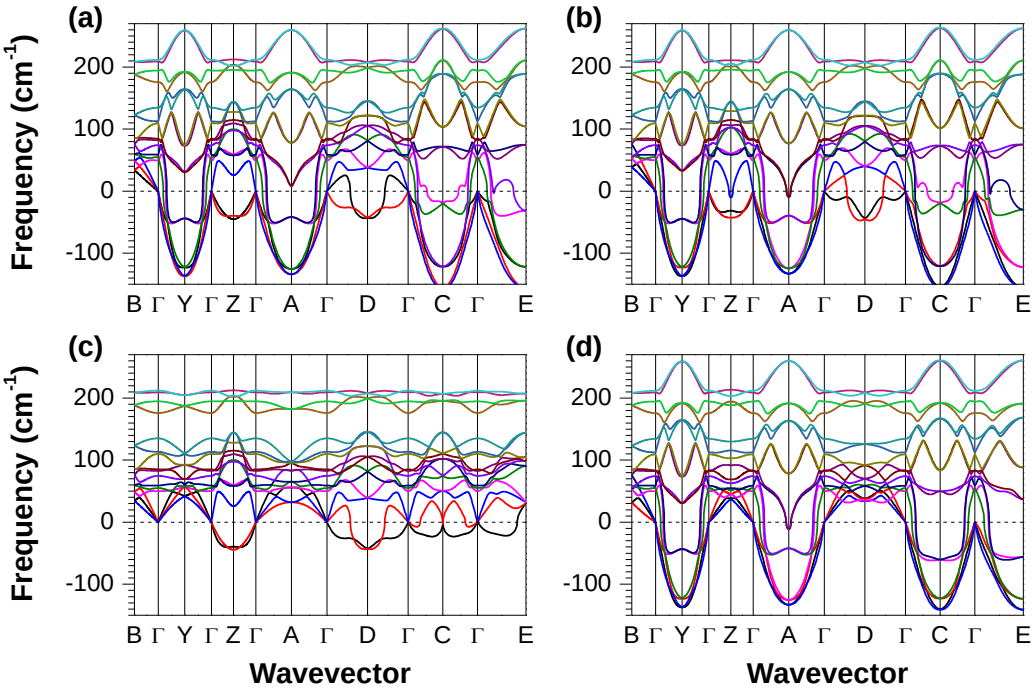

Figure S1. Phonon dispersions calculated by using (a) the normal unit cell, and (b) 2×1×1, (c) 1×2×1, and (d) 1×1×2 supercells. The *k*-points of high symmetry in the first Brillouin zone are labeled as follows: B = (0.5, 0, 0), Γ = (0, 0, 0), Y = (0, 0.5, 0), Z = (0, 0, 0.5), A = (0.5, 0.5, 0), D = (0.5, 0, 0.5), C = (0, 0.5, 0.5), E = (0.5, 0.5, 0.5).

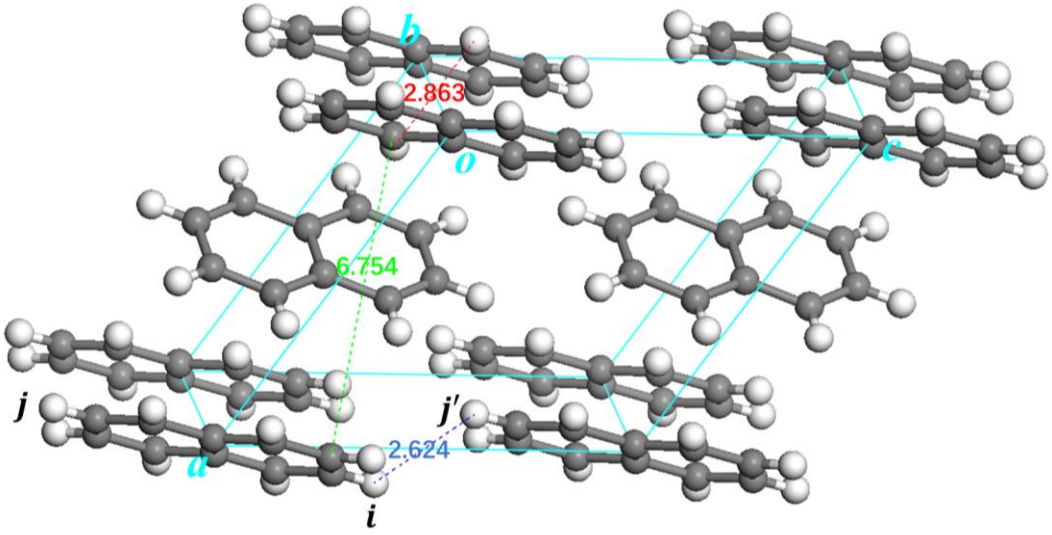

Figure S2. Illustration of the shortest inter-atomic distances between adjacent equivalent molecules along the a- (green), b- (red), and c-axes (blue). As an example, atom j' is the atom equivalent to atom j in the adjacent unit cell along c-axis. When atoms j and j' are displaced simultaneously, atom i will feel forces from both atoms j and j' via intra- and inter-molecular interactions, respectively.

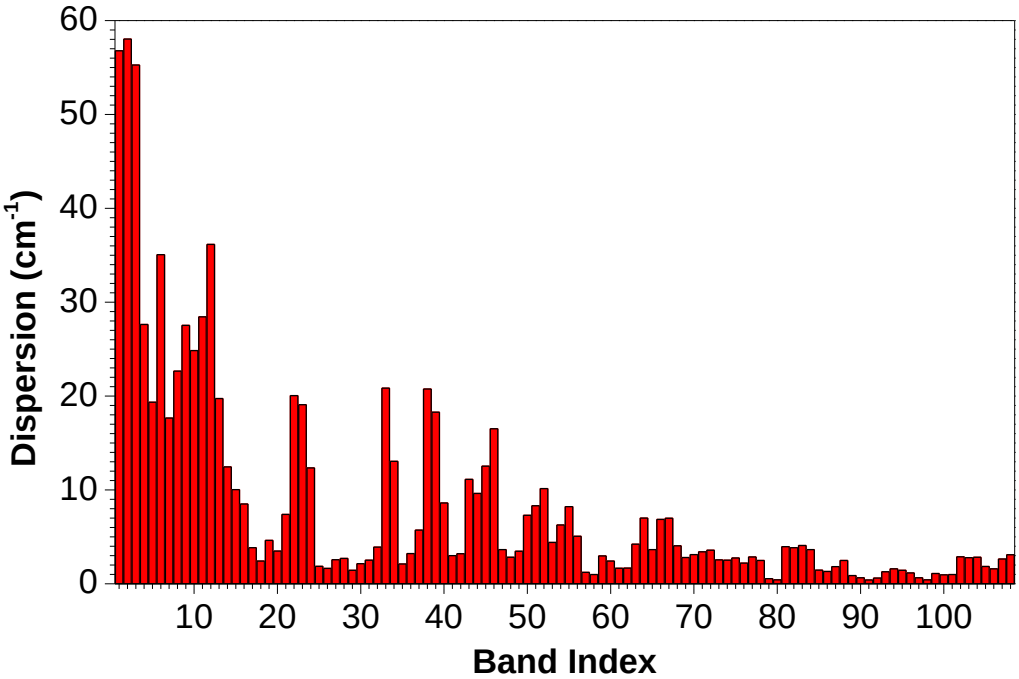

Figure S3. Dispersions of all phonon branches.

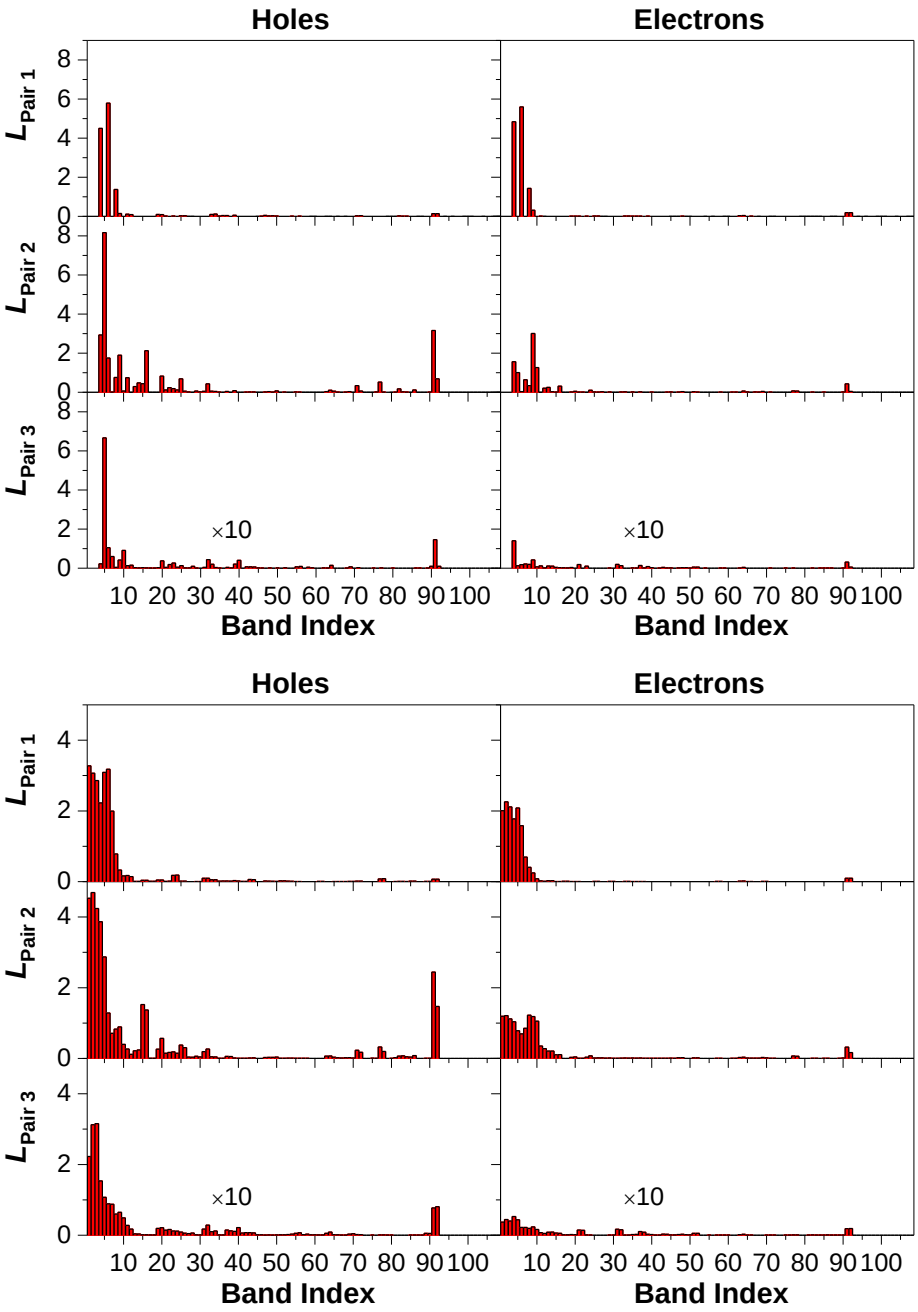

Figure S4. Contributions of each phonon branch to L ($\sum_{\boldsymbol{k},s}\frac{v^2(\boldsymbol{k},j,s)}{2\hbar\omega(\boldsymbol{k},j)}$) for holes and electrons (in meV) obtained by using 1×1×1 (upper panel) and 8×8×8 (bottom panel) *k*-point meshes.

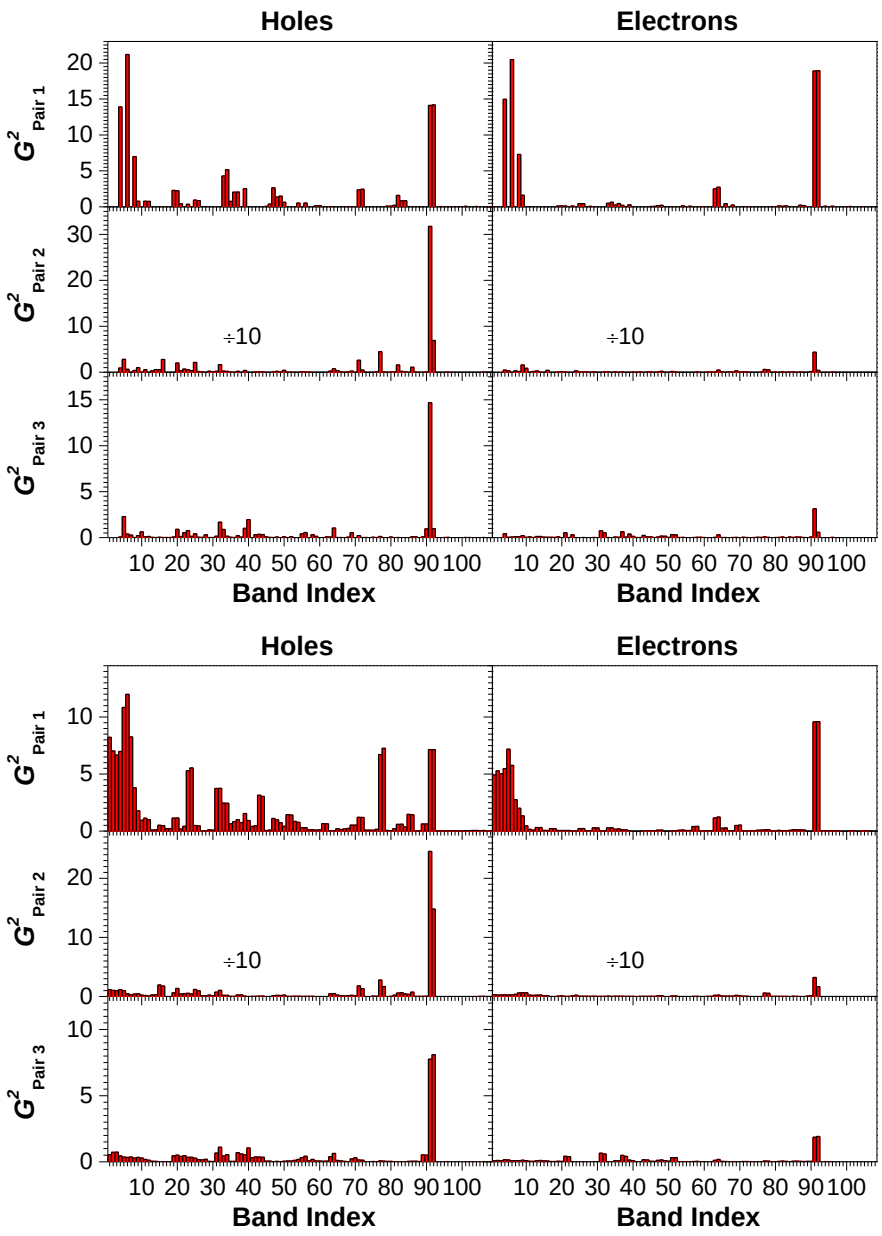

Figure S5. Contributions of each phonon branch to the G^2 parameters for holes and electrons (in meV^2) obtained by using $1\times1\times1$ (upper panel) and $8\times8\times8$ (bottom panel) *k*-point meshes.

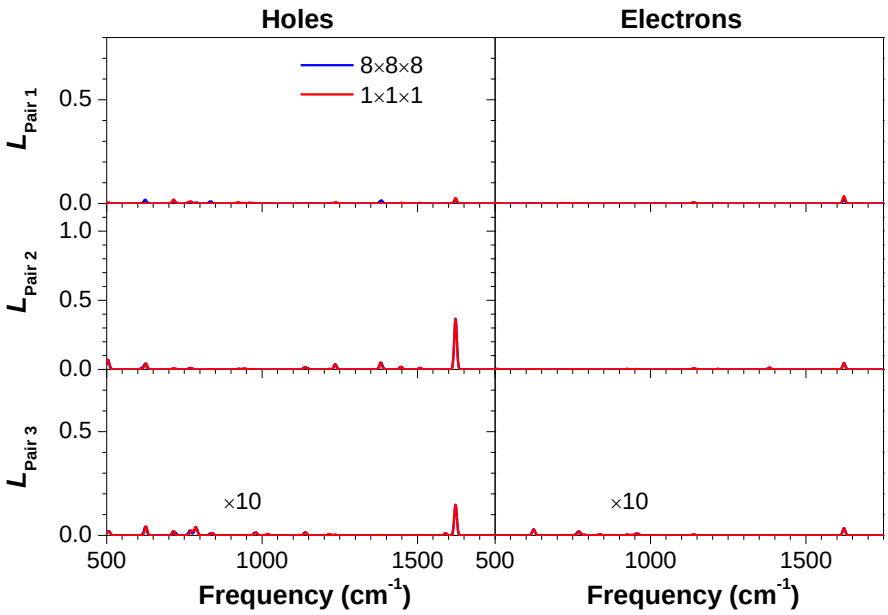

Figure S6. Dependence of L on phonon frequencies. The plots are obtained by replacing the delta functions in $L = \sum_{\boldsymbol{k},j,s} \frac{v^2(\boldsymbol{k},j,s)}{2\hbar\omega(\boldsymbol{k},j)} \delta[\omega - \omega(\boldsymbol{k},j)]$ by Gaussian functions with a full width at half-maximum (FWHM) of 10 cm^{-1}.

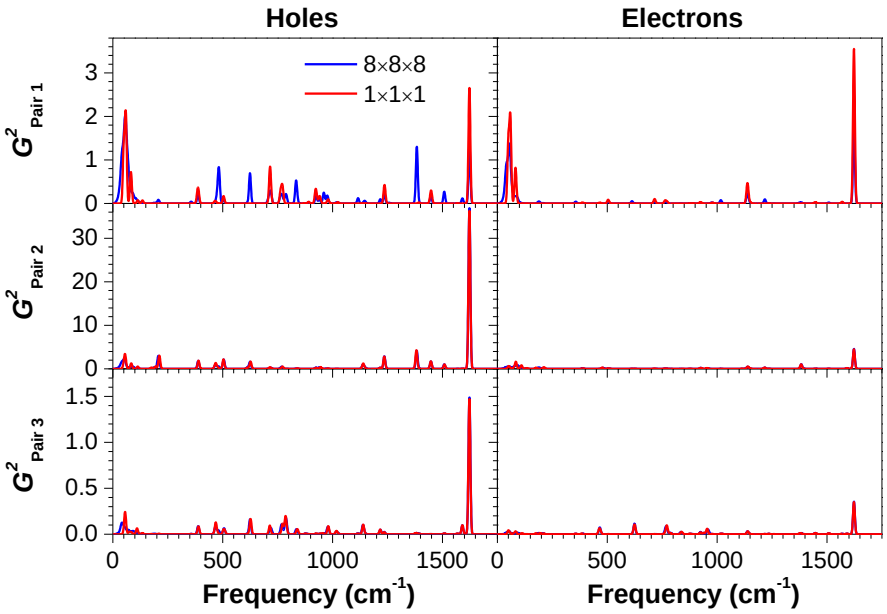

Figure S7. Dependence of G^2 on phonon frequencies. The plots are obtained by replacing the delta functions in $G^2 = \sum_{\boldsymbol{k},j,s} \frac{v^2(\boldsymbol{k},j,s)}{2} \delta[\omega - \omega(\boldsymbol{k},j)]$ by Gaussian functions with a full width at half-maximum (FWHM) of 10 cm^{-1}.

Table S1. PHONOPY estimates of the frequencies (in cm^{-1}) of all vibration modes derived at the Γ-point.

index	frequency	index	frequency	index	frequency	index	frequency
1	0	28	510	55	979	82	1447
2	0	29	612	56	981	83	1449
3	0	30	614	57	1016	84	1451
4	50	31	622	58	1016	85	1507
5	55	32	627	59	1022	86	1509
6	59	33	714	60	1026	87	1568
7	74	34	717	61	1115	88	1570
8	82	35	761	62	1115	89	1590
9	84	36	764	63	1136	90	1591
10	110	37	770	64	1139	91	1622
11	113	38	772	65	1141	92	1623
12	135	39	773	66	1143	93	3098
13	176	40	786	67	1149	94	3099
14	194	41	789	68	1151	95	3100
15	209	42	791	69	1217	96	3101
16	212	43	837	70	1217	97	3110
17	355	44	842	71	1235	98	3110
18	358	45	877	72	1238	99	3111
19	385	46	891	73	1255	100	3111
20	390	47	922	74	1260	101	3119
21	463	48	927	75	1374	102	3120
22	468	49	940	76	1375	103	3120
23	469	50	945	77	1381	104	3120
24	477	51	954	78	1383	105	3124
25	503	52	955	79	1393	106	3125
26	504	53	972	80	1394	107	3125
27	509	54	977	81	1443	108	3128

Table S2. Estimates of $t^{(0)}$ and G for holes and electrons (in meV) for various k-point meshes of phonons.

	Holes			Electrons		
	Pair 1	Pair 2	Pair 3	Pair 1	Pair 2	Pair 3
				$t^{(0)}$		
INDO	-35.9	-4.0	12.4	9.3	28.8	-1.4
PBE	-31.6	-9.4	13.9	14.0	39.9	-3.7
B3LYP	-35.1	-10.3	15.5	16.1	44.9	-4.2
				G		
1×1×1	10.7	26.9	6.0	9.7	11.8	3.4
1×1×2	10.8	27.1	6.0	9.8	12.1	3.4
1×2×1	12.4	27.1	6.0	8.3	11.9	3.4
2×1×1	10.7	27.2	6.1	9.7	11.9	3.4
2×2×2	12.5	27.3	6.1	8.4	12.0	3.4
2×2×4	12.5	27.2	6.1	8.3	12.0	3.4
2×4×2	12.6	27.3	6.1	8.4	12.0	3.4
4×2×2	12.5	27.3	6.1	8.4	12.0	3.4
4×4×4	12.6	27.3	6.1	8.4	12.0	3.4
4×4×8	12.6	27.3	6.1	8.4	12.0	3.4
4×8×4	12.7	27.3	6.1	8.4	12.0	3.4
8×4×4	12.6	27.3	6.1	8.4	12.0	3.4
8×8×8	12.7	27.3	6.1	8.4	12.0	3.4